INTERNATIONAL JOURNAL FOR NUMERICAL METHODS IN FLUIDS, VOL. 13, 699–711 (1991)

BOUNDARY LINEAR INTEGRAL METHOD FOR COMPRESSIBLE POTENTIAL FLOWS

Z. FANG AND I. PARASCHIVOIU

Department of Mechanical Engineering, Ecole Polytechnique de Montreal, Montreal, Quebec, Canada

SUMMARY

A boundary linear integral method based on Green function theory has been developed to solve the full potential equation for subsonic and transonic flows. In this integral method, potential values in the flow region are determined by potential values represented by boundary integrals and a volume integral. The boundary potential values are obtained by implementing the boundary integrals along boundary segments where a linear potential relation is assumed. The volume integral is evaluated in a grid generated by finite element discretization. The volume integral is evaluated only outside the body. Therefore there is no extra boundary treatment required for evaluation of the volume integral. The source term is assumed to be constant in an element integral volume. The volume integral needs to be evaluated only once and can be stored in computer memory for further usage.

KEY WORDS Boundary linear Integral method Shock integrals

INTRODUCTION

The integral method for solving partial differential equations is a very useful tool in computational fluid dynamics. This method provides an alternative approach to the finite difference and finite element methods for solving transonic potential flows. One of the advantages of the integral method is that it can be easily applied to solve flow problems over complex configurations. A major technical obstacle involved with other methods seems to be the difficulty in generating suitable grids for flows with complex configurations.[1] In the integral method the computational grids include two parts: boundary grids and field grids. Boundary grids are used for implementation of the boundary integrals while field grids are used for evaluation of certain volume integrals instead of the conventional purpose of replacing partial differential equations. Therefore many kinds of grids can be adopted for field grids required by the integral method.

Another advantage of the integral method is that solutions can be obtained by only using surface panels, and solutions everywhere else can be represented by the solutions on surface panels. For non-linear equations, only the discretized simultaneous equations for surface points are solved in iterative solution procedures. Generally, the number of grid points on surfaces is much smaller than the number of grid points in the field. Thus the integral method could take less computer CPU time.

Computational schemes based on the integral formulation have been developed for the linear Prandtl–Glauert equation.[2,3] More recently, the full potential equation has been solved using the integral method.[4–12] Application of the integral method to solve the unsteady potential equation has been studied.[13,14] The full potential equation has also been solved using the integral method for flows over multielement aerofoils[15] and over the entire aircraft.[16,17] For transonic flows, some

0271–2091/91/160699–13$06.50

Received October 1989
Revised November 1990

methods combine the integral method with the finite volume method[5] while other methods use the integral method incorporated with the finite difference method.[7] It is not clear how these methods treat the shock integrals resulting from the Green function transformation.

In this paper the exact integral method is applied to solve the full potential equation for compressible flows. The boundary linear integral method[18] is used in this work. The coefficient matrix is formulated on body grid points only. The non-linear full potential equation is solved by a Newton–Raphson iteration procedure. In each iteration the influence matrix does not change and needs to be decomposed only once. Only the source term in the volume integral needs to be evaluated in each iteration. After potential values on the body have been obtained, potential values anywhere else can be calculated. For transonic flows, shock integrals are calculated and contributions are added to the right-hand side of the discretized simultaneous equations. Our results show that shock integrals are necessary for capturing sharp shock jumps.

In this work, two-dimensional flows over the NACA 0012 aerofoil are calculated. Numerical results are compared with experimental data.[19] The good agreement between numerical results and experimental data shows that the boundary linear integral method provides an alternative tool for analytical and design purposes in aeronautical engineering.

GOVERNING EQUATION AND BOUNDARY CONDITIONS

In Cartesian co-ordinates the conservative form of the full potential equation is

$$\nabla\cdot(\rho\nabla\Phi)=0, \tag{1}$$

where Φ is the full potential, ρ is the density and ∇ is defined by

$$\nabla=\frac{\partial}{\partial x}\hat{i}+\frac{\partial}{\partial y}\hat{j}+\frac{\partial}{\partial z}\hat{k}. \tag{2}$$

The full potential equation given by (1) is not very suitable for integral representation because the left-hand side of this equation is not a Laplacian operator. However, the full potential equation can be written in the alternative form

$$\nabla^2\Phi=\sigma. \tag{3}$$

The source term σ is expressed by

$$\sigma=M^2\Phi_{ss}, \tag{4}$$

where M is the Mach number Φ_{ss} is the rate of velocity change along the streamline direction.

The boundary condition of equation (1) at infinity is given by

$$\Phi_\infty=V_\infty(x\cos\alpha+y\sin\alpha). \tag{5}$$

The surface boundary conditions for inviscid flows are the tangential flow conditions given by

$$\mathbf{n}\cdot\nabla\Phi=0, \tag{6}$$

where $\mathbf{n}$ is the normal vector on the body surface. The Kutta condition is also implemented, which requires that the flow leaves the trailing edge smoothly.

In this work the superimposition principle is used to solve equation (3). The solution of this equation has two parts, Φ_1 and Φ_2. Φ_1 is the harmonic solution and Φ_2 is the unharmonic solution. Thus the solution of equation (3) can be represented by

$$\Phi=\Phi_1+\Phi_2 \tag{7}$$

and the Laplacian operation is

$$\nabla^2\Phi=\nabla^2\Phi_1+\nabla^2\Phi_2. \tag{8}$$

Since Φ_1 is harmonic and Φ_2 is unharmonic, Φ_1 satisfies the Laplace equation and Φ_2 satisfies the Poisson equation. Therefore equation (3) can be decomposed into two equations:

$$\nabla^2\Phi_1=0, \tag{9}$$

$$\nabla^2\Phi_2=\sigma. \tag{10}$$

In this work Φ_1 is solved by using the routine linear potential panel method[18] and Φ_2 is obtained by the field boundary linear integral method. After decomposition of the partial differential equation, a set of decomposed boundary conditions is also required. The boundary conditions at infinity can be decomposed as

$$\Phi_{1\infty}=V_\infty(x\cos\alpha+y\sin\alpha), \tag{11}$$

$$\Phi_{2\infty}=0. \tag{12}$$

Considering equations (6) and (7), the tangential condition on the body surface can also be decomposed. Substituting equation (7) into equation (6), we have

$$\mathbf{n}\cdot\nabla\Phi=\mathbf{n}\cdot\nabla\Phi_1+\mathbf{n}\cdot\nabla\Phi_2=0. \tag{13}$$

Since Φ_1 is the incompressible potential flow solution, Φ_1 must satisfy the tangential condition on the body surface

$$\mathbf{n}\cdot\nabla\Phi_1=0. \tag{14}$$

Therefore

$$\mathbf{n}\cdot\nabla\Phi_2=0. \tag{15}$$

The Kutta condition can also be decomposed in the same way.

The Laplace equation for Φ_1 is solved only once and the Poisson equation can be solved iteratively. Solutions are assumed to be obtained when the iterative procedure converges.

INTEGRAL FORMULATION

The integral methods are based on Green's theory. One of the useful formulations is the second Green identity[20] which is

$$\iint_\Omega(\Phi\nabla^2\Phi_L-\Phi_L\nabla^2\Phi)\,d\Omega=-\int_\Gamma\left(\Phi\frac{\partial\Phi_L}{\partial\mathbf{n}}-\Phi_L\frac{\partial\Phi}{\partial\mathbf{n}}\right)ds. \tag{16}$$

The necessary condition for this integral transformation is that the potential Φ is continuously differentiable and has continuous partial derivatives of the second order in region Ω. In transonic flows, shocks are present in the flow region. Across shocks, both the first- and second-order derivatives of the potential are not continuous. Therefore, in order to satisfy the continuity condition requirement of the potential derivatives, the boundary of the region Ω must include the shocks, and the resulting boundary integrals along shocks are called shock integrals.

Using Green's theorem, Φ_1 can be represented by the sum of boundary integrals,

$$\Phi_1(x_p,y_p)=\oint[(\mathbf{n}\cdot\nabla\Phi_1)\Phi_L-\Phi_1(\mathbf{n}\cdot\nabla\Phi_L)]\,ds, \tag{17}$$

and Φ_2 can be represented by the sum of boundary integrals and a volume integral,

$$\Phi_2(x_p, y_p)=\oint [(\mathbf{n}\cdot\nabla\Phi_2)\Phi_L-\Phi_2(\mathbf{n}\cdot\nabla\Phi_L)]\,ds+\int_V \sigma\Phi_L\,dV, \tag{18}$$

where the surface integral is on boundaries of a single connected region and the volume integral is inside the region. $\Phi_1(x_p, y_p)$ and $\Phi_2(x_p, y_p)$ are decomposed potential values at an arbitrary location P inside the region or on the boundary. For two-dimensional problems Φ_L is given by

$$\Phi_L=\frac{1}{2\pi}\ln[(x-x_p)^2+(y-y_p)^2]^{0.5}. \tag{19}$$

In equations (17) and (18) the boundary integrals include those at infinity. When a numerical procedure is employed, it is inconvenient to perform the integrals at infinity directly. However, integrals at infinity can be transformed into a simple solution called the undisturbed potential by using Green function theory. The undisturbed potential is defined by

$$\Phi_f=V_\infty(x\cos\alpha+y\sin\alpha). \tag{20}$$

The undisturbed potential satisfies the Laplace equation $\nabla^2\Phi=0$ everywhere and also satisfies the boundary condition at infinity. Considering a region surrounded by a boundary at infinity and applying Green function theory to the undisturbed potential, we have

$$\Phi_f(x_p, y_p)=\oint_\infty [(\mathbf{n}\cdot\nabla\Phi_f)\Phi_L-\Phi_f(\mathbf{n}\cdot\nabla\Phi_L)]\,ds. \tag{21}$$

Thus integrals at infinity in equation (17) can be represented by the undisturbed potential Φ_f and integrals at infinity in equation (18) disappear because $\Phi_{2\infty}$ is equal to zero as determined by the boundary condition decomposition. By substituting the undisturbed potential into equation (17) and $\Phi_{2\infty}=0$ into equation (18), solutions can be expressed by

$$\Phi_1(x_p, y_p)=\Phi_f+\int_{B+C} [(\mathbf{n}\cdot\nabla\Phi_1)\Phi_L-\Phi_1(\mathbf{n}\cdot\nabla\Phi_L)]\,ds, \tag{22}$$

$$\Phi_2(x_p, y_p)=\int_{B+C+SH} [(\mathbf{n}\cdot\nabla\Phi_2)\Phi_L-\Phi_2(\mathbf{n}\cdot\nabla\Phi_L)]\,ds+\int_V \sigma\phi_L\,dV, \tag{23}$$

where B represents body surfaces, C denotes wakes or cuts between region boundaries and SH is along shock waves. On body surfaces and wakes we have

$$\int_{B+C} (\mathbf{n}\cdot\nabla\Phi_1)\Phi_L\,ds=0, \tag{24}$$

$$\int_{B+C} (\mathbf{n}\cdot\nabla\Phi_2)\Phi_L\,ds=0, \tag{25}$$

because of the tangential boundary conditions. Across shocks we have

$$\int_{SH} \Phi_2(\mathbf{n}\cdot\nabla\Phi_L)\,ds=0, \tag{26}$$

since the tangential velocities are assumed to be equal across shock waves. Thus equations (17) and (18) become respectively

$$\Phi_1(x_p, y_p)=\Phi_f-\int_B \Phi_1(\mathbf{n}\cdot\nabla\Phi_L)\,ds-\Gamma_1\int_C (\mathbf{n}\cdot\nabla\Phi_L)\,ds, \tag{27}$$

$$\Phi_2(x_p, y_p) = -\int_B \Phi_2(\mathbf{n}\cdot\nabla\Phi_L)\,ds - \Gamma_2\int_C (\mathbf{n}\cdot\nabla\Phi_L)\,ds + \int_{SH}(\mathbf{n}\cdot\nabla\Phi_2)\Phi_L\,ds + \int_V \sigma\Phi_L\,dV, \tag{28}$$

where

$$\Gamma_1 = \Phi_{1+} - \Phi_{1-}, \tag{29}$$

$$\Gamma_2 = \Phi_{2+} - \Phi_{2-}, \tag{30}$$

with Φ_{1+}, Φ_{1-} and Φ_{2+}, Φ_{2-} potential values across the wake. The total circulation is

$$\Gamma = \Gamma_1 + \Gamma_2, \tag{31}$$

which is determined from the solutions.

NUMERICAL PROCEDURE

In equation (27) potential values everywhere are represented by boundary integrals and in equation (28) potential values are represented by boundary integrals plus an extra volume integral. For incompressible flows the source term σ is zero and there is no shock. Thus only Φ_1 is solved. The incompressible potential depends only on the boundary integrals on the body surface and the wake. If the potential values on the body surface are determined, potential solutions everywhere can be calculated. For compressible flows the source term has to be evaluated and, if supersonic flow appears, shock integrals have to be performed.

To determine the potential solution on the body surface, equations (27) and (28) are applied to points on the body surface. Therefore the body surface needs to be discretized into many pieces of small panels. Applying the surface integrals to each panel will result in a system of simultaneous equations. The potential solutions on the body surface are obtained from solutions of these simultaneous equations. Within a boundary segment a linear potential formulation is assumed,

$$\Phi = \Phi_1 + \frac{\xi}{l}(\Phi_{i+1} - \Phi_i), \tag{32}$$

where l is the segment length and ξ varies from zero to l. Applying the integral equations on the body surface and introducing this linear potential relation into these boundary integrals, a set of linear simultaneous equations results:

$$[A_{i,j}][\Phi_i] = [F_i] \tag{33}$$

where $i = 1, \ldots, m$ and $j = 1, \ldots, m$, with m the total number of nodes on boundaries. For both decomposed potentials Φ_1 and Φ_2 the matrix [A] is identical. Thus this matrix needs to be decomposed only once.

For compressible flows the source term must be evaluated throughout the volume. For transonic flows the integral for shocks is needed because the normal derivative of potential across a shock wave is discontinuous. In this work, potential values across shock waves are assumed to be continuous because the tangential velocities across shocks are equal.

The volume integral in equation (28) is evaluated in a field grid obtained by finite element discretization. In each element volume the source term inside the volume integral is assumed to be constant. Thus

$$\int_V \sigma\Phi_L\,dV = \sum_1^M \sigma_i \int_{V_i} \Phi_L\,dV. \tag{34}$$

The integral $\int_{v_i} \Phi_L\,dV$ can be calculated analytically and the results are given in the form of a limit

function which can be called in the main programme. Formulations are derived in the Appendix at the end of this paper.

RESULTS AND DISCUSSION

The solution procedure discussed above was applied to compressible flows over the NACA 0012 aerofoil for a range of Mach numbers from subsonic to transonic flows. Numerical results are compared with experimental data.[19]

Numerical solutions are obtained on a grid generated by finite element discretization with 1176 element and 1275 nodes. The boundary grid consists of 30 panels on the upper surface and 30 panels on the lower surface, with most panels near the leading and trailing edges. A wake network consisting of two panels in the boundary grid is appended to the trailing edge of the aerofoil. The wake is aligned with the chord disector. The wake panels are divided into 11 smaller grid segments when building up the field grid. The boundary of the field grid is located at a distance of six chord lengths around the aerofoil. Beyond that the source distributions are small and can therefore be neglected.

The non-linear potentials are solved by an iterative procedure. First, the linear Laplace equation for incompressible flows is solved. Thus the source distribution can be evaluated. The iterative solution procedure is performed by using the first-evaluated source distribution. In each iteration a system of simultaneous equations on the boundary grid is solved and then the source distribution is calculated inside the field grid. If supersonic flow appears, shock integrals are calculated. The contributions of the volume and shock integrals are added to the right-hand side of the system equations. Because the matrix of the system equations does not change in the iteration loops, the matrix is decomposed in advance only once to speed up the solution. The iteration number for subsonic flows is in the range 7–10 for the system residual to reach the order of 10^{-8}. For transonic flows, more iterations are needed to reach the same system residual order.

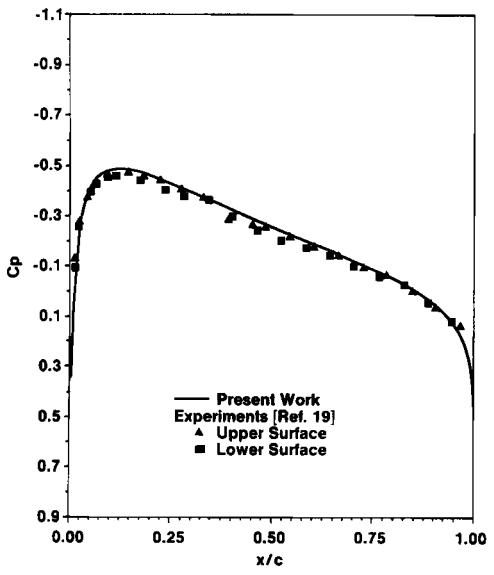

Figure 1. Pressure coefficient for NACA 0012 aerofoil; $M_\infty = 0{\cdot}5$, $\alpha = 0°$

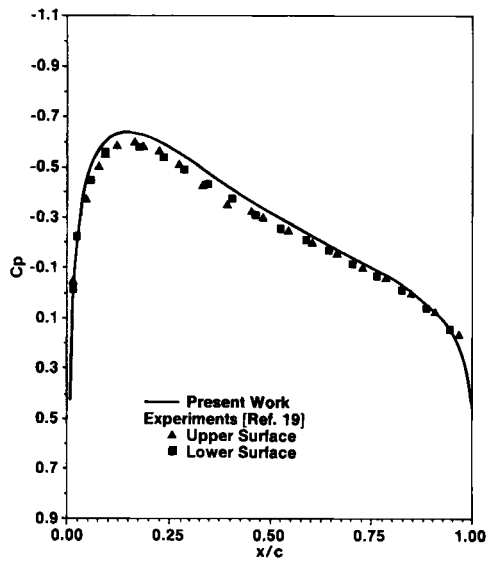

Figure 2. Pressure coefficient for NACA 0012 aerofoil; $M_\infty = 0{\cdot}7$, $\alpha = 0°$

For flows with a Mach number of 0·8 at infinity and a 0° angle of attack the number of iterations is about 35.

In Figures 1 and 2, pressure coefficients for compressible flows over the NACA 0012 aerofoil with Mach numbers of 0·5 and 0·7 at infinity respectively and a 0° angle of attack are presented. Good agreement between numerical results and experimental data in these cases is shown. In Figure 3, pressure coefficients for flow over the NACA 0012 aerofoil with a Mach number of 0·5 at

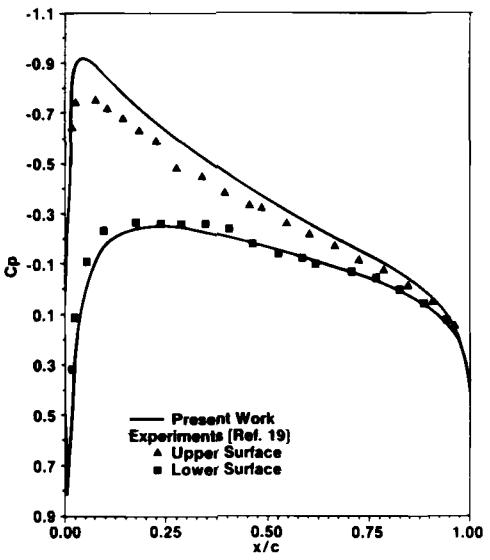

Figure 3. Pressure coefficient for NACA 0012 aerofoil; $M_\infty = 0{\cdot}5$, $\alpha = 2°$

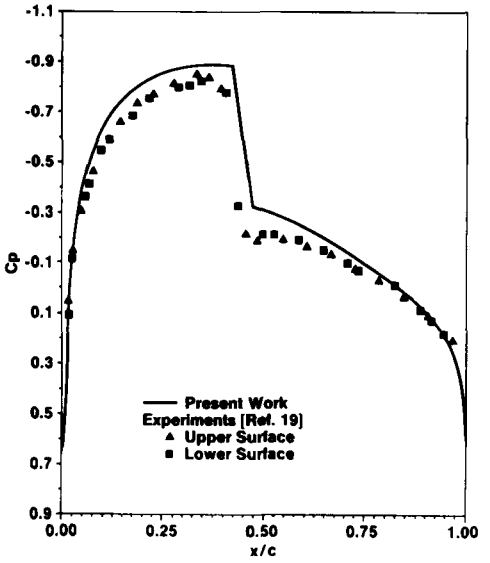

Figure 4. Pressure coefficient for NACA 0012 aerofoil; $M_\infty = 0{\cdot}8$, $\alpha = 0°$

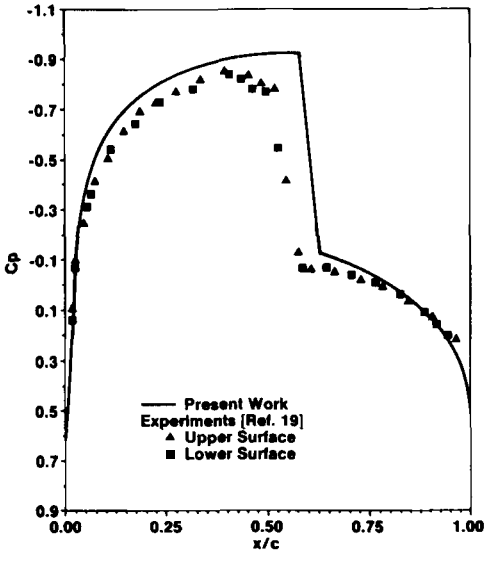

Figure 5. Pressure coefficient for NACA 0012 aerofoil; $M_\infty = 0{\cdot}83$, $\alpha = 0°$

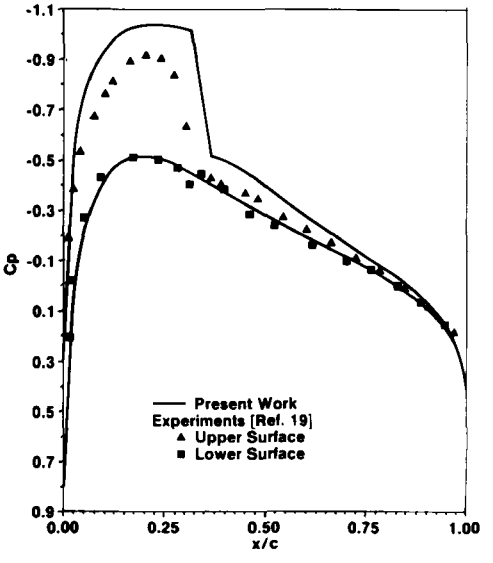

Figure 6. Pressure coefficient for NACA 0012 aerofoil; $M_\infty = 0{\cdot}75$, $\alpha = 1°$

infinity and an angle of attack of 2° are presented. The numerical results predict lower pressure coefficients along the upper surface of the aerofoil. Pressure coefficients for flows over NACA 0012 with Mach numbers of 0·8 and 0·83 at infinity and a 0° angle of attack are shown in Figures 4 and 5 respectively. The numerical solutions are fairly close to the experimental data in these cases. Pressure coefficients for a Mach number of 0·75 at infinity and angles of attack of 1°

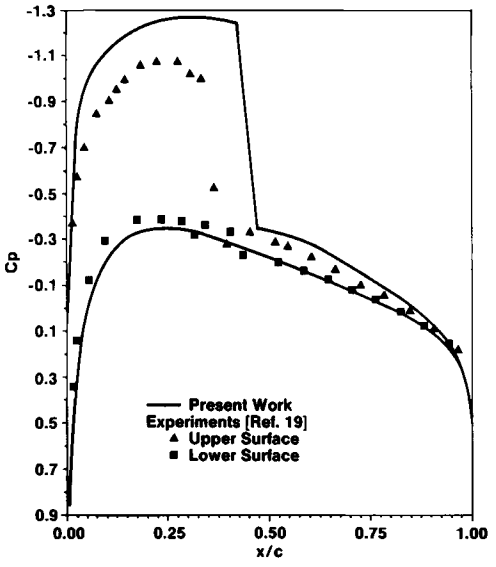

Figure 7. Pressure coefficient for NACA 0012 aerofoil; $M_\infty = 0{\cdot}75$, $\alpha = 2°$

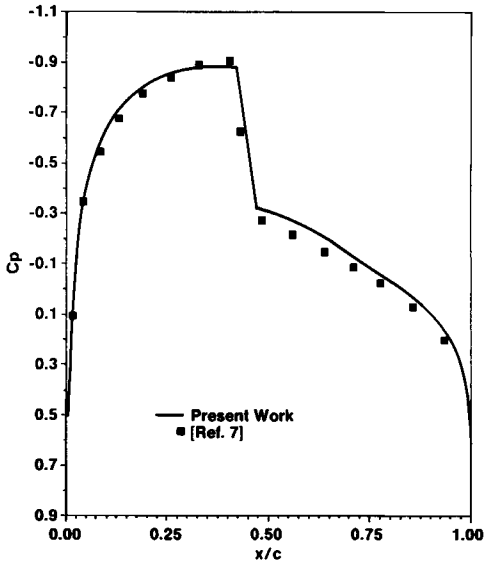

Figure 8. Pressure coefficient for NACA 0012 aerofoil; $M_\infty = 0{\cdot}8$, $\alpha = 0°$

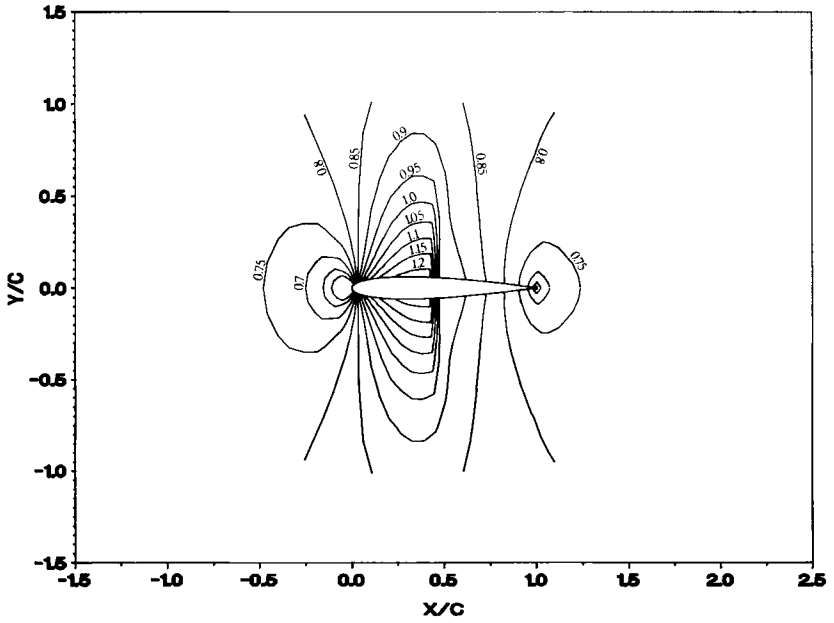

Figure 9. Iso-Mach lines; $M_\infty = 0{\cdot}8$, $\alpha = 0°$

and 2° are shown in Figures 6 and 7 respectively. In the lifting case the numerical solutions predict lower pressure coefficients on the upper surface of the aerofoil.

In Figure 8, pressure coefficients obtained in this work are compared with the numerical results provided in Reference 7 for flows with a Mach number of 0·8 and a 0° angle of attack. Our results

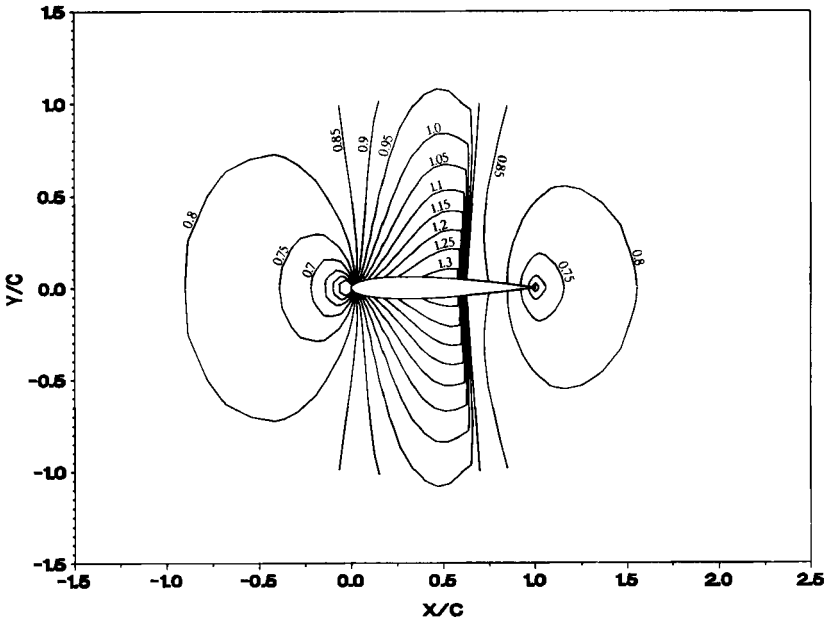

Figure 10. Iso-Mach lines; $M_\infty = 0{\cdot}83$, $\alpha = 0°$

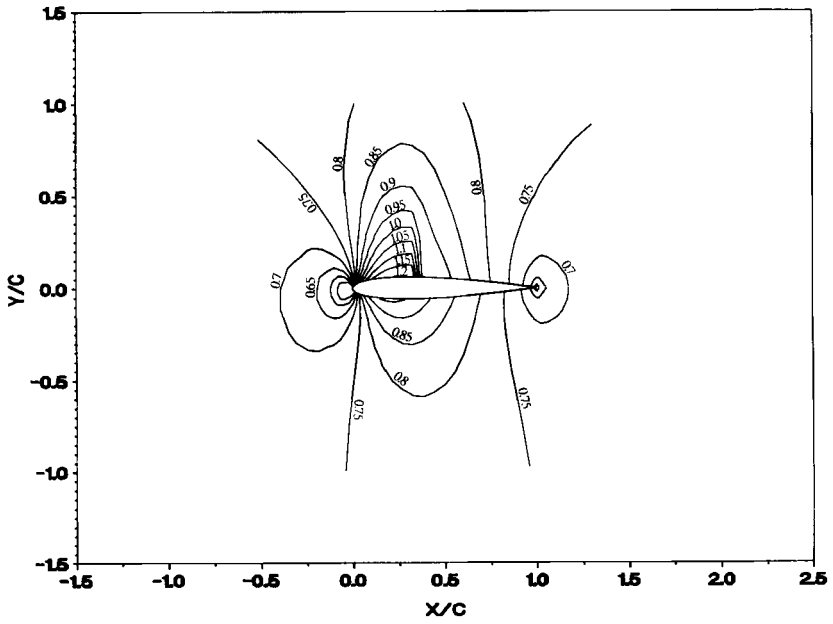

Figure 11. Iso-Mach lines; $M_\infty = 0{\cdot}75$, $\alpha = 1°$

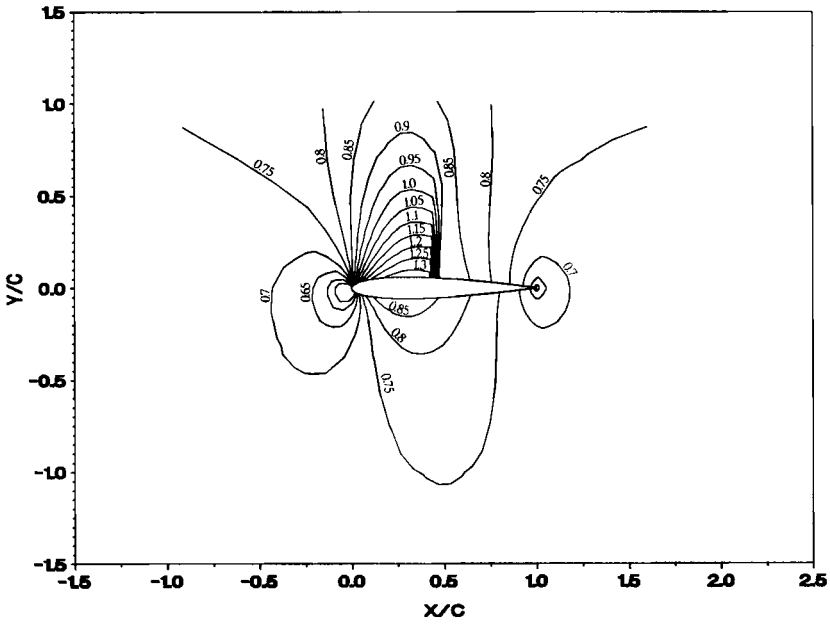

Figure 12. Iso-Mach lines; $M_\infty = 0{\cdot}75$, $\alpha = 2^\circ$

are close to the results of Reference 7 obtained by a finite difference approach for the shock calculation. In the integral formulation of Reference 7 the shock integral does not appear. Therefore the difference scheme has to be incorporated with the integral approach because the iterative procedure for subsonic flows does not converge for transonic flows. In this work, shock integrals are performed explicitly and artificial viscosities studied in Reference 3 are added in supersonic regions.

In Figures 9 and 10, iso-Mach lines for Mach numbers of 0·8 and 0·83 respectively and an angle of attack of 0° are presented. Iso-Mach lines for a Mach number of 0·75 and angles of attack of 1° and 2° are shown in Figures 11 and 12 respectively. In these figures the shock regions are relatively thick owing to the grid size near the shock. In the present work there is no grid clustering used near the shock regions.

CONCLUDING REMARKS

The numerical study in this work shows that the boundary linear integral method provides an alternative approach for solving transonic potential flow problems. With this method the full potential equation is solved only on the body surface. The potential solutions in the entire flow field are represented by the solutions on the body surface and are used for calculating the source distribution. Since the number of grid points on the body surface is much smaller than that in the entire flow field, the requirement for computer CPU time is reduced.

With the boundary linear integral method the grid system is divided into two parts: surface grids and field grids. The surface grids are used to obtain the potential solution on the surface and the field grids are used to calculate the source distribution and the field integral. Since there is no specific requirement for the field grids, many kinds of grid can be adopted by the boundary integral method. Thus this method eliminates the difficulty in grid generation encountered in other field methods.

In this work the shock integrals generated by Green function theory are performed explicitly when the flow is transonic. Our results show that the shock integrals are necessary to capture sharp shock jumps. In this approach the contribution of the shock integrals is added to the right-hand side of the discretized simultaneous equations. This approach is a shock-capturing method because there is no requirement for preknown shock locations. The numerical results compare fairly well with the experimental data.

APPENDIX

The volume integral given by equation (34) is calculated analytically and the results are presented as a limit function which can be written as a standard function in a FORTRAN programme.

Assume the element integral volume boundaries can be represented by

$$y=a+bx. \tag{35}$$

Introducing $\bar{x}=x-x_p$ and $\bar{y}=y-y_p$, the boundary equation becomes

$$\bar{y}=A+B\bar{x}, \tag{36}$$

where

$$A=a-y_p+bx_p, \tag{37}$$

$$B=b. \tag{38}$$

The element volume integral becomes

$$\int_{V_i}\Phi_L\,dV=\frac{1}{2\pi}\int_{\bar{x}_A}^{\bar{x}_B}\left(\int_{\bar{y}_L}^{\bar{x}_U}\ln(\bar{x}^2+\bar{y}^2)\,d\bar{y}\right)d\bar{x}, \tag{39}$$

where

$$\bar{x}_A=x_A-x_p, \tag{40}$$

$$\bar{x}_B=x_B-x_p, \tag{41}$$

$$\bar{y}_U=A_U+B_U\bar{x}, \tag{42}$$

$$\bar{y}_L=A_L+B_L\bar{x}. \tag{43}$$

In equations (42) and (43) the subscript U represents the upper boundaries and L denotes the lower boundaries. Carrying out the integration, we can obtain the limit function of the volume integral

$$\begin{aligned}F(\bar{x})=&(A\bar{x}+0{\cdot}5B\bar{x}^2)\ln[(1+B^2)(\bar{x}+2B_1\bar{x}+C_1)]+\bar{x}^2\tan^{-1}\frac{A+B\bar{x}}{\bar{x}}\\&-\frac{B(C_1+2B_1^2)-2AB_1D_1}{2}\ln(\bar{x}^2+2B_1\bar{x}+C_1)+\frac{A(C_1-2B_1^2)D_1+2BB_1^3}{E_1}\tan^{-1}\frac{\bar{x}+B_1}{E_1}\\&-1{\cdot}5B\bar{x}^2+(BB_1-2A)\bar{x}-AD_1\bar{x},\end{aligned} \tag{44}$$

where

$$B_1=\frac{AB}{1+B^2}, \tag{45}$$

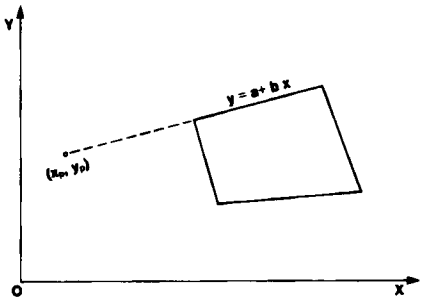

Figure 13. Volume integration when $A=0$

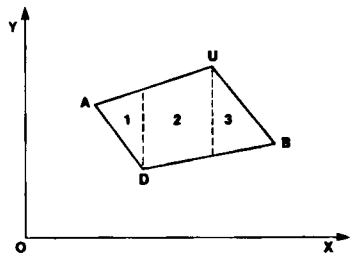

Figure 14. Volume integration by subregions

$$C_1=\frac{A^2}{1+B^2}, \tag{46}$$

$$D_1=\frac{1+2B^2}{1+B^2}, \tag{47}$$

$$E_1=\frac{A}{1+B^2}. \tag{48}$$

If $A=0$, the singularity location (x_p, y_p) is on the line represented by $y=a+bx$ as shown in Figure 13. The limit function becomes

$$F(\bar{x})=0{\cdot}5B\bar{x}^2\ln[(1+B^2)\bar{x}^2]-1{\cdot}5B\bar{x}^2+\bar{x}^2\tan^{-1}B. \tag{49}$$

If the singularity location (x_p, y_p) is on the node point of the finite integral volume, $x=x_p$ and $y=y_p$. Thus the limit function value becomes zero.

The value of a volume integral is obtained by calling the limit functions. In Figure 14, a typical finite integral volume is shown. The integral region is divided into three subregions. In region 1 the integral value is

$$I_1=F_{AU}(\bar{x}_D)-F_{AD}(\bar{x}_D)-[F_{AU}(\bar{x}_A)-F_{AD}(\bar{x}_A)], \tag{50}$$

in region 2 we have

$$I_2=F_{AU}(\bar{x}_U)-F_{DB}(\bar{x}_U)-[F_{AU}(\bar{x}_D)-F_{DB}(\bar{x}_D)], \tag{51}$$

while in region 3

$$I_3=F_{UB}(\bar{x}_B)-F_{DB}(\bar{x}_B)-[F_{UB}(\bar{x}_U)-F_{DB}(\bar{x}_U)]. \tag{52}$$

The integral value in this integral volume is

$$I=I_1+I_2+I_3. \tag{53}$$

Special care should be taken when the finite integral volume appears to be different from the one shown in Figure 14. However, the limit function form remains the same.

REFERENCES

1. T. L. Holst, J. W. Slooff, H. Yoshihara and W. F. Ballhaus Jr., *Applied Computational Transonic Aerodynamics*, in B. M. Spee and H. Yoshihara (eds), *AGARD-AG-266*, 1982, p. 86.

2. K. Tseng and L. Morino, 'Nonlinear Green's function methods for unsteady transonic flows', in D. Nixon (ed.), *Transonic Aerodynamics*, AIAA, New York, 1982, pp. 565–603.
3. W. J. Piers and J. W. Slooff, 'Calculation of transonic flow by means of a shock-capturing field panel method', *Proc. AIAA Computational Fluid Dynamics Conf.*, 1979, *AIAA paper 79-1459*, pp. 147–156.
4. F. T. Johnson, R. M. James, J. E. Bussoletti and A. C. Woo, 'A transonic rectangular grid embedded panel method', *AIAA paper 82-0953, AIAA/ASME 3rd Joint Thermophysics, Fluids, Plasma and Heat Transfer Conf.*, St. Louis, MO, 7–11 June 1982.
5. B. Oskam, 'Transonic panel method for the full potential equation applied to multicomponent airfoils', *AIAA J.*, **23**, 1327–1334 (1985).
6. J. C. Crown, 'Calculation of transonic flow over thick airfoils by integral methods', *AIAA J.*, **6**, 413–423 (1968).
7. P. M. Sinclair, 'An exact integral (field panel) method for the calculation of two-dimensional transonic potential flow around complex configurations', *The Aeronaut. J.*, (June/July), **90**, 227–236 (1986).
8. O. A. Kandil and H. Hu, 'Full-potential integral solution for transonic flows with and without embedded Euler domains', *AIAA J.*, **26**, 1079–1086 (1988).
9. C. Masson, 'Panel method for transonic flows', *M.Sc. Thesis*, Ecole Polytechnique de Montreal, 1989.
10. L. L. Erickson, and S. M. Strande, 'A theoretical basis for extending surface-paneling methods to transonic flow', *AIAA J.*, **23**, 1860–1867 (1985).
11. L. Chu, E. Yates and O. Kandil, 'Integral equation solution of the full potential equation for transonic flows', *AIAA paper 89-0563, AIAA 27th Aerospace Sciences Meeting*, Reno, NV, 9–12 January 1989.
12. D. E. Wilson, 'A new singular integral method for compressible potential flow', *AIAA paper 85-0481, AIAA 23rd Aerospace Sciences Meeting*, Reno, NV, 14–17 January 1985.
13. M. H. L. Hounjet, 'Transonic panel method to determine loads on oscillating airfoils with shocks', *AIAA J.*, **19**, 559–566 (1981).
14. M. H. L. Hounjet, 'A field panel/finite difference method for potential unsteady transonic flow', *AIAA J.*, **23**, 537–545 (1985).
15. N. D. Halsey, 'Calculation of compressible potential flow about multielement airfoils using a source field-panel approach', *AIAA paper 85-0038, AIAA 23rd Aerospace Sciences Meeting*, Reno, NV, 14–17 January 1985.
16. L. L. Erickson, M. D. Madson and A. C. Woo, 'Application of the TranAir full-potential code to the F-16A', *J. Aircraft*, **24**, 540–545 (1987).
17. P. M. Sinclair, 'A three-dimensional field-integral method for the calculation of transonic flow on complex configurations—theory and preliminary results', *The Aeronuat. J.*, (June/July), **92**, 235–243 (1988).
18. J. Moran, *Theoretical and Computational Aerodynamics*, Wiley, New York, 1984.
19. J. J. Thibert, M. Grandjacques and L. H. Ohman, 'NACA-0012 airfoil, an experimental data base for computer program assessment', *AGARD-AR-138*, 1979, pp. A1.1–A1.10.
20. O. D. Kellogg, *Foundations of Potential Theory*, Dover, New York, 1953, pp. 211–277.